

Cardiac Arrhythmia, CHF, and NSR Classification With NCA-Based Feature Fusion and SVM Classifier

Deepak H. A., SJB Institute of Technology, India

Vijayakumar T., SJB Institute of Technology, India

ABSTRACT

An arrhythmia is an irregular heartbeat that causes abnormal heart rhythms. Manual analysis of electrocardiogram (ECG) signals is not sufficient to quickly detect cardiac arrhythmias. This study proposes a deep learning approach based on a convolutional neural network (CNN) architecture for the classification of cardiac arrhythmias (ARR), congestive heart failure (CHF), and normal sinus rhythm (NSR). First, the ECG signal is converted into a 2D image using time-frequency conversion. The scalogram is constructed using a continuous wavelet transform to extract dynamic features. With CNN, each ECG signal is broken down into heartbeats, and then each heartbeat is converted into a 2D grayscale image of the heartbeat. Morphological feature extraction was performed by segmenting the QRS complex and detecting P and T waves. A third approach to feature extraction is dual-tree complex wavelet transform (DT-CWT). In addition, all extracted features are combined using neighborhood component analysis (NCA), and features are selected to classify using a support vector machine (SVM) classifier.

KEYWORDS

CNN, CWT, DCWT, ECG, NCA, PCA, QRS, SVM

INTRODUCTION

The working principle of the tissues and organs in our body is based on the potential difference that occurs as a result of the electrochemical events of the cells. This potential difference produces electrical signals that can be measured from the body surface. The electrical activity of the heart is also measured and evaluated by the electrocardiography (ECG) method. ECG is the recording of the potential difference that occurs due to the contraction and relaxation of the heart during a heartbeat with the help of electrodes placed on the body surface. In a healthy person's ECG signal, there are P waves, QRS complexes, and T waves, each representing different phases of the heartbeat. Analysis and interpretation of ECG signals recorded for a certain period of time play an important role in the diagnosis of any heart-related disease. Abnormalities caused by the wave formation time, shape or the time difference between the waves cause arrhythmic heart rhythms (Xiong et al., 2018). Early and accurate diagnosis of arrhythmic signals is critical in preventing diseases that may result in sudden death.

Manual analysis of the ECG signal is not sufficient for rapid detection of abnormalities in heart rhythm. The analysis of the long-term ECG signal by the experts takes a lot of time and this analysis

DOI: 10.4018/IJSI.315659

This article published as an Open Access article distributed under the terms of the Creative Commons Attribution License (<http://creativecommons.org/licenses/by/4.0/>) which permits unrestricted use, distribution, and production in any medium, provided the author of the original work and original publication source are properly credited.

may not accurately identify the problem. Computer-aided decision systems are being developed in the examination of ECG signals due to its advantages such as increasing the accuracy of diagnosis, shortening the analysis time, and reducing the expert errors that may occur. In the literature, there are many different studies based on signal processing methods related to arrhythmia detection using ECG signals. These studies are based on the extraction of different features from the signals and the classification of these features.

Depending on the examination of the time or frequency domain, ECG morphology (Anwar et al., 2018), RR interval (Xiang et al., 2018), principal component analysis (PCA) (Manik et al., 2019), independent component analysis (ICA) (Desai et al., 2015), Fourier transform (Kurniawan et al., 2020), empirical mode decomposition (EMD) (Izci et al., 2018), The features are extracted by methods such as discrete wavelet transform (DWT) (Hamed & Owis, 2016; Chen & Maharatna, 2020). Different machine learning algorithms are used in the classification of feature vectors obtained from arrhythmic and normal signals. Support vector machines (SVM) (Li et al., 2020), k-nearest neighbor (k-NN) classifier (Qaisar et al., 2020), artificial neural networks (ANN) (Dewangan & Shukla, 2016; Subbiah & Subramanian, 2018) are among the classifiers used in the classification of ECG signals. In traditional machine learning algorithms, the signals go through the preprocessing stage in order to decompose the noise that may occur during signal recording. At this stage, the signal is cleared of noise by various filters. Deep learning algorithms are being developed as an alternative to machine learning algorithms consisting of preprocessing, feature extraction and classification stages. Deep learning can perform preprocessing, feature extraction and classification stages together, thanks to many hidden layers in its structure (Hatami et al., 2018).

In this paper contribution are as follows,

An Alexnet-NCA-SVM hybrid structure is suggested for Arrhythmia, CHF, and NSR ECG signal categorization. The proposed method is implemented with hybridization of time frequency scalogram images to get deep features, Morphological features, DTCWT and PCA features fused with NCA to demonstrate its superiority in classifier. This paper's contribution to the literature can be summarized as follows. ECG signals for arrhythmia, CHF, and NSR are grouped together. The Alexnet-NCA-SVM hybrid structure was used for classification.

The rest of this paper is structured as follows. The second section presents Literature review; third section represents proposed method for classifying the proposed ECG signals. Fourth section discusses the simulation results in the MATLAB environment. The fifth section contains a final commentary with instructions for further work.

LITERATURE REVIEW

In recent studies on the classification of arrhythmic signals, deep learning methods are preferred because of their high success (Ullah et al., 2020). These methods vary according to the training model they use. Recurrent neural networks (RNN) (Zhang et al., 2020; Pokaparakarn et al., 2022; Hannun et al., 2019), deep neural networks (DNN) (Nonaka & Seita, 2020; Jun et al., 2018), convolutional neural networks (CNN) (Kiranyaz et al., 2016) are examples of these models.

A model for diagnosing cardiac arrhythmias was proposed by Singh and Singh (2019) with filter-based feature selection approaches were applied to three separate machine learning algorithms applied to the Cardiac Arrhythmia data set, and the best features were picked. The performance of feature selection approaches was assessed using SVM, random forest. Isin and Ozdalili (2017) proposed a deep learning-based technique for classifying patient ECG's and automating ECG arrhythmia detection. AlexNet feature descriptor is used in the proposed method. To reach the final classification, the retrieved characteristics are fed into a simple back propagation neural network. To test the suggested approach, three class different ECG waveforms were chosen from the MIT-BIH Arrhythmia database. The results show that the deep learning feature can reach very high-performance

rates when combined with a typical back propagation neural network. While the highest accuracy rate of 98.51 percent was achieved, test accuracy was approximately 92 percent.

Bulbul et al. (2017) employed machine learning approaches to classify P, Q, R, S, and T waves in ECG signals using MLP and SVM techniques. Alarsan and Younes (2019) proposed a machine learning-based ECG categorization strategy based on multiple ECG characteristics. These characteristics are machine learning algorithm inputs, and a total of 205,146 data points were collected. For classification, such as Decision Trees, Random Forests, and Gradient Boosted Trees (GDB) were employed. The approach has an overall accuracy of 96.75 percent using the GDB Tree algorithm and 97.98 percent using random Forest for binary classification, according to the findings.

Sharma et al. (2020) Classified ECG signals using the LSTM model. First, ECG data were used to compute RR-interval sequences. After that, using Fourier-Bessel (FB) expansion, the property vector was extracted from the RR interval sequences. The LSTM model is used to classify the obtained vectors. The MIT-BIH Arrhythmia Data Set was employed for classification, and accuracy was 90.07 percent with ten-fold cross validation. Masetic and Subasi (2016) developed a classifier based on characteristics derived from the ECGs of 13 healthy CHF patients and 15 CHF patients. They used Random Forests, SVM, C4.5, ANN, and k-NN approaches to obtain excellent accuracy. Isler (2016) Used heart rate variability (HRV) analysis to distinguish between patients with systolic and diastolic congestive heart failure (CHF).

CNN is a very popular model in studies of classification of ECG signals. First, authors of Huang et al. (2019) introduced the structure using the single-layer CNN model for arrhythmia classification. In addition to using the CNN model for one-dimensional signals, it is also used to classify 2-dimensional images. In these studies, pictures obtained from ECG signals are given as input data to the CNN model (Goldberger et al., 2000). Considering the success of the model in picture classification, high success was achieved by converting and classifying the signals into pictures (Vieau & Iaizzo, 2015).

PROPOSED METHODOLOGY

In this paper, the ECG signals from three PhysioNet databases (Pereira et al., 2020) are taken for various feature extraction operations which will be explained in the subsequent subheadings.

In the proposed system, as seen in figure 1, the ECG signal scalogram does not need any preprocessing and feature extraction as ECG signals are converted into scalogram images for deep feature extraction. Further in the other sections ECG signals are preprocessed and Morphological features, DTCWT features and PCA features are extracted. The proposed system creates the hybridization of Deep features and hand-crafted features with NCA (Neighborhood component analysis) to create hybrid set of features for classification using SVM. There are three class classification as class label ARR, CHF, NSR.

Electrocardiogram

When an action potential is conducted through the myocardium during the cardiac cycle, an electric current is generated, which is recorded by an electrocardiograph through electrodes placed on the surface of the body. These electrodes record the sum of all action potentials emitted by the heart at any given time. The summed recording of cardiac action potentials results in an ECG (Dössel et al., 2021).

Although this test is not a direct measurement of mechanical events in the heart and cannot be used to infer muscle contraction force and blood pressure, any abnormalities in the ECG recording are indicative of electrical events associated with a mechanical event. Thus, the ECG is the most widely used biomedical signal in the clinical diagnosis of the heart due to its easy, non-invasive and painless recording.

A normal ECG consists of a P wave, a QRS complex, and a T wave as seen in Figure 2.

The sample time between onset of P and onset of QRS complex is the PR interval. At the end of PR interval ventricles begin to depolarize. The QT interval is the time where ventricles contract and relax (Goldberger et al., 2018).

Figure 1. Block diagram for proposed methodology

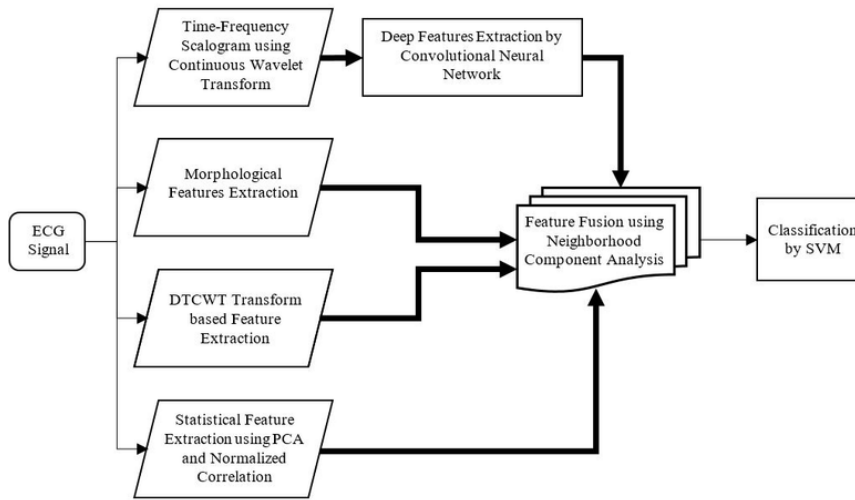
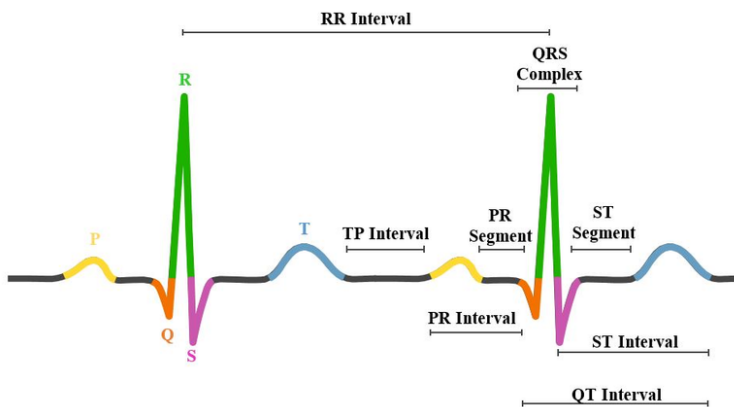


Figure 2. Electrocardiogram with waves, segments, intervals and segment marked (Goldberger et al., 2018)



The ECG can be recorded as the potential difference between a negative and a positive pole (Kusumoto & Bernath, 2012). ECG represented in to frontal leads, which use extreme electrodes and measure electrical activity in the vertical plane; and the anterior leads, use six-chest electrodes to measure electrical activity in the horizontal plane. As shown in figure 3(a), the three leads are marked by Roman numerals - I, II and III - and consist of a bipolar lead, as they are marked by possible differences between the two ends. The three wires are designated by Roman numerals - I, II and III - and consist of two-pole wires, as they are indicated by the potential difference between the two ends. The other three in the frontal plane refer to unipolar leads or augmented leads (aVR, aVL and aVF), as shown in figure 3(b). They are called unipolar leads due to the recording of electrical potentials at a location in relation to an electrode with an action potential close to zero (Singh & Majumder, 2019).

In the precordial leads, electrical activity is measured between one of the six chest electrodes and the sum of signals from the left and right arms and the left leg, which usually has a value close to zero. Figure 4(a) shows the relative position of each electrode in the thorax and Figure 4(b) the spatial relationship of the six thoracic leads that record the electrical voltages transmitted in the horizontal plane (Dössel et al., 2021).

Figure 3. Representation of the electrodes used to obtain the frontal ECG leads: (a) I, II, III, (b) aVR, aVL and aVF (Kusumoto & Bernath, 2012)

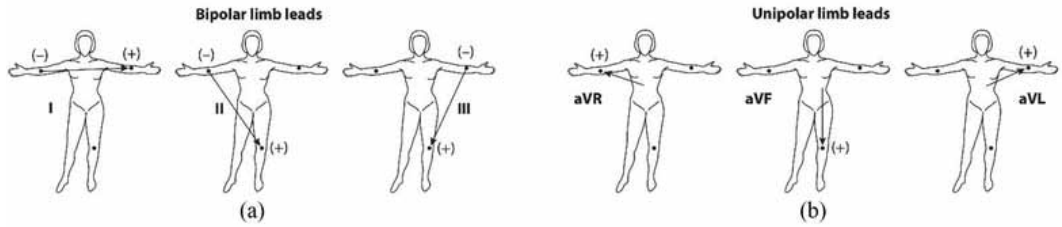
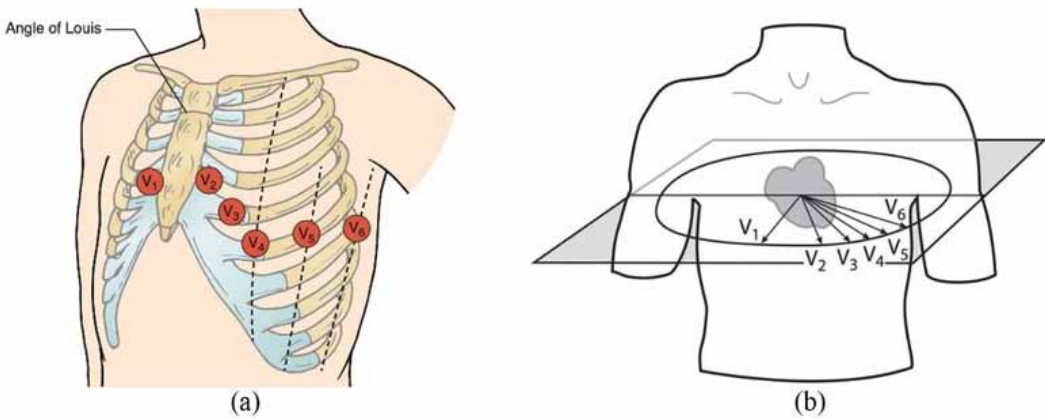


Figure 4. (a) Location of electrodes relative to precordial leads (Dössel et al., 2021) (b) Representation of the horizontal plane formed by the chest leads (Kusumoto & Bernath, 2012)



Time-Frequency Transform for Scalogram

Initial Considerations

The ECG signals are electrical signals produced by the heart to stimulate the heart muscles during the operation of the heart and show the electrical activity of the heart. Continuous recording and evaluation of ECG signs during the monitoring of heart diseases, determination of appropriate diagnosis and treatment, and monitoring of the applied treatment are very important in terms of determining the abnormalities and complications that may occur. In general, the monitoring of machines and equipment is performed by obtaining the vibration signals of the machine operating at a constant speed, which characterizes this signal as stationary, that is, its frequency components do not vary with time. In this case, the Fourier transform can be used as a tool to study the spectral characteristics of the signal in the frequency domain.

In more complex situations, the signals may present non-stationary characteristics, such as ECG signals and vibration signals in rotating machines with variable rotation. In these cases, it becomes more appropriate to analyze the behaviour of the variation of spectral components over time.

It is for this purpose that the so-called time-frequency transforms (TFDs) are applied to the analysis of machines and equipment aiming at fault detection and diagnosis. One of the advantages of using TFDs for machine monitoring is that they tell you when and how the frequency content of the signal is changing. The wavelet transform (WT) is one such tool. It has the advantage of presenting a noble resolution in the time-frequency plane, but it has the disadvantage of incorporating interference terms when signals with more than one spectral component are analyzed.

Another widely used distribution is the Short Term Fourier Transform (STFT). This technique comprises of separating the non-stationary signal into intervals small enough so that stationarity can be assumed in each of them, and thus the Fourier transform can be applied with good results. The sum of the spectra for each interval shows how the frequency composition of the signal changes over time. The signal splitting is done through the use of an observation window to emphasize the signal characteristics only in the vicinity of the instant of interest.

One of the limitations of STFT concerns the window width, which is fixed for all times. According to the Heisenberg uncertainty principle, large windows provide good resolution in the frequency domain, poor resolution in the time domain, and vice versa. In this way, the information obtained by STFT has limited accuracy due to the width of the window.

To solve the fixed (scale) resolution problem of the STFT, a transform that is independent of the scale can be used, that is, that presents the characteristic of multiresolution. This transformation is known as continuous wavelet transform (CWT), and allows you to analyze the signal with time resolution or frequency, depending on the width of the selected window (Wang et al., 2021).

Next, some concepts, theoretical aspects and information about the CWT are presented.

Continuous Wavelet Transform

The wavelet transform represents an advance over STFT, as it is a method which uses variable scales. For the higher resolution at high frequency signal in wavelet analysis uses smaller scale and for low frequency signal where greater resolution is required uses larger scale. Hence frequency and scale are inversely proportional, where higher scale implies low frequency and vice versa.

The CWT is the time scale decomposition of signal and it can be mapped through scalogram. It is similar to time-frequency mapping with STFT. In fact, there is a correspondence between scale and frequency, which is why several authors consider the Wavelet Transform to be a time-frequency representation. The wavelet transform consists of finding a family of functions called daughter wavelets, based on dilation and translation operations of the mother wavelet, as will be seen later. There are many types of Wavelets that can be used as a mother wavelet, they are Haar's Wavelet, Meyer's Wavelet, Coiflet's Wavelet, Morlet's Wavelet, Daubechies' Wavelet, etc. These Wavelets have different characteristics. In this work, the Daubechies Wavelets are used.

The Continuous Wavelet Transform (CWT) of the signal $x(t)$ is defined by (Wang et al., 2021):

$$CWT(a,b) = \frac{1}{\sqrt{a}} \int_{-\infty}^{\infty} x(t) \cdot \Psi\left(\frac{t-b}{a}\right) dt \quad (1)$$

Where, $\Psi(t)$ symbolizes the mother wavelet and $\Psi\left(\frac{t-b}{a}\right)$ are the daughter wavelets. The parameter a is called a scale, which modifies the length of a function by compression or dilation; b is a translation factor that predicts or delays the position of the wavelet on the time axis.

The main difference between STFT and WT is that WT uses a scale variable "a", instead of the frequency variable "f", in STFT. The values of the continuous wavelet transform obtained from equation (1) is called the wavelet coefficient, which is a function of position and scale.

Deep Features Extraction by Convolutional Neural Network

Deep learning (DL) is a Machine learning (ML) technique that imparts computers to perform tasks that are natural to humans, such as learning from examples, so that they can solve problems such as image and speech recognition. This technique is increasingly being applied to the biological sciences (Yıldırım et al., 2018).

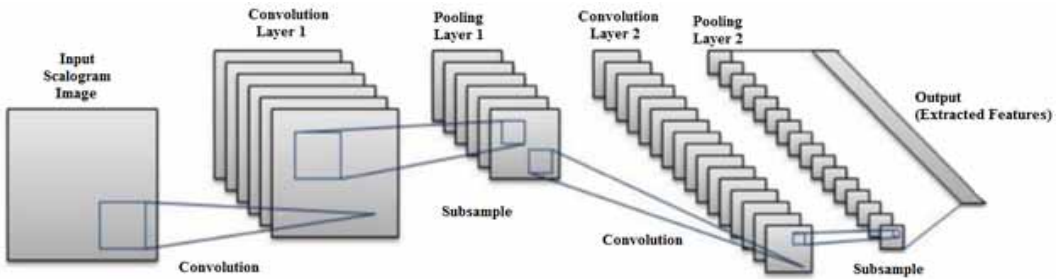
Given a large dataset, DL models are considered a good approach and often exceed human agreement rates. In line with what was mentioned above, the DL has been demonstrating recognition accuracies never before achieved (Yıldırım et al., 2018).

Deep learning techniques can reveal invisible image features from original images. Convolutional Neural Network (CNN) has proven to be very useful for feature extraction and learning and have been used in many studies (Zhao et al., 2020). With the advancement of deep learning technology in recent years, more efficient CNN (DCNN) models have been proposed such as VGG, AlexNet, ResNet, DenseNet, and EfficientNet. This deep CNN performs well in image classification tasks and allows computers to outperform humans in visual classification.

In this study, a deep CNN model was applied that can extract feature vectors of scalogram images. As shown in Figure 5 in the basic architecture of CNN, features were extracted from scalogram input images with successive convolution and pooling layers in CNN. At this stage, the established model and CNN are mentioned.

A convolution set (convolution-pooling) is made that separates and defines various features of the scalogram image and this process is called feature extraction.

Figure 5. Architecture for deep convolutional neural network (Zhao et al., 2020)



Convolutional Layer

The feature extraction phase similar to the stimulation process in cells of the visual cortex. This phase consists of a combination of periodic layers of evolving neurons and descending pattern neurons. As the data progresses through this phase, the levels of the layers decrease, making them less sensitive to input changes, but at the same time increasing the complexity of the resources. A building block consists of one or more:

- Convolutional layer (CONV) that processes data from a receiving field.
- Correction layer (ReLU), often called “ReLU” with reference to the activation function (rectified linear unit);
- Pooling layer (POOL) is the compression of information by reduction of the dimensions of the intermediate image (often by subsampling). The typical architecture of CNN is shown in figure 5.

With deep learning approach input is normally represented as vector of different dimension (tensor) and the kernel is often represented as multi dimension vectors. As an example, if input is image I then kernel will be 2-dimension structure (Dössel et al., 2021) which is denoted as K , in equation (2):

$$S(i, j) = (I * K)(i, j) = \sum_m \sum_n I(i - m, j - n) K(m, n) \quad (2)$$

Morphological Features Extraction

Morphological features carry information about the shape of both the entire ECG as a whole and the P-QRS-T intervals that form it. In order to complete the ECG signal segmentation procedure, detection of all its other characteristic waves (P, Q, S, and T) is therefore necessary.

Segmentation of QRS Complexes

After the exact detection of the positions of the QRS complexes, we seek to identify all its elementary waves (the Q wave and the S wave) and also its start and end points (QRS_on and QRS_off). The extraction of its characteristic points is very complicated because of the wide variation in the morphology of QRS complexes.

In this work, the segmentation of QRS complexes relies on the determination of the slope of the filtered signal using the three-point derivation method, expressed in equation (3) (Goldberger et al., 2018):

$$f'(x) \approx \frac{f(x+h) - f(x-h)}{2h} \quad (3)$$

Where f symbolizes the denoised signal the time division is represented by h .

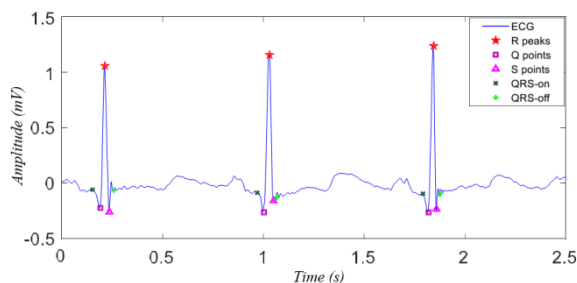
Q Wave Detection: In order to extract the position of the Q peak, it is based on the fact that the maximum possible duration of the QRS complex is equal to 160 ms. In this case, we consider a window extending from the position point of the peak R to the left with 80 ms. Then, the Q wave is extracted by performing in this window the search for the first point verifying the sign inversion of the slope expressed in equation (4) (Yücelbaş et al., 2018):

$$f'(i) * f'(i-1) < 0 \quad (4)$$

S Wave Detection: The extraction of the S wave is carried out in such a way that the detection of the Q wave by considering a window of 80 ms in width. However, this time the window is positioned to the right of peak R.

Detection of characteristic points QRS_on and QRS_off: The start and end points of the QRS complexes correspond respectively to the points having a minimum value of the slope (almost zero) because the Q and S waves are low amplitude components. Therefore, the search for these two characteristic points (QRS_on and QRS_off) is carried out before the Q wave and after the S wave in a window of 40 ms. Figure 6 illustrates the location of the Q and S waves and the points marking the start and end of the QRS complexes for the '100' record.

Figure 6. Representation of the characteristic points of the QRS complexes of the recording '100'



Detection of P and T Waves

The positions of the P and T waves are looked for in the interval between two consecutive QRS complexes [QRS_off (j): QRS_on (j + 1)], where j indicates the current pulse rate. First, we divided this interval by 2/1. Then, the maximum position in the first field is subtracted as the position of the peak T and the position of the peak P is determined as the position of the maximum in the second field.

The results of the detection of all the characteristic waves of the recordings '101' and '205' are shown respectively in figure 7 and figure 8.

Figure 7. Representation of all detected waves of record '101'

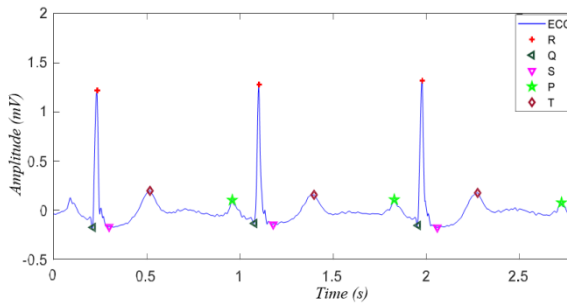
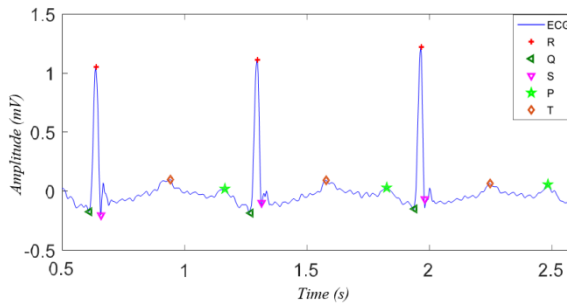


Figure 8. Representation of all detected waves of record '205'



DT-CWT based Feature Extraction

The DT-CWT was proposed to represent an improvement of the DWT transform, as it provides information on the magnitude of the non-oscillating coefficients at points close to singularities, approximate invariance to signal displacement, less aliasing effect and greater directional selectivity. Furthermore, DT-CWT allows the signal to be perfectly reconstructed from its wavelet representation, has limited redundancy and still has linear phase (Wang et al., 2021).

Similar to sinusoidal Fourier basis functions, a complex wavelet function is defined in equation (5):

$$\Psi_c(t) = \Psi_h(t) + j\Psi_g(t) \quad (5)$$

Where $\Psi_h(t)$ represents the real (even) part, $j\Psi_g(t)$ represents the imaginary (odd) part, and $j = \sqrt{-1}$. It is important to define the functions representing the real and imaginary part as a Hilbert

pair $(\mathcal{H})(\Psi_h(t))$ and $\Psi_g(t)$ must have a phase shift of 90° from each other) so that $\Psi_c(t)$ is an analytical signal and present the characteristics of the Fourier transform.

The complex coefficient $d_c(s, t) = d_h(s, t) + jd_g(s, t)$ has magnitude defined in equation (6):

$$|d_c(s, t)| = \sqrt{[d_h(s, t)]^2 + [d_g(s, t)]^2} \tag{6}$$

And phase defined in equation (7):

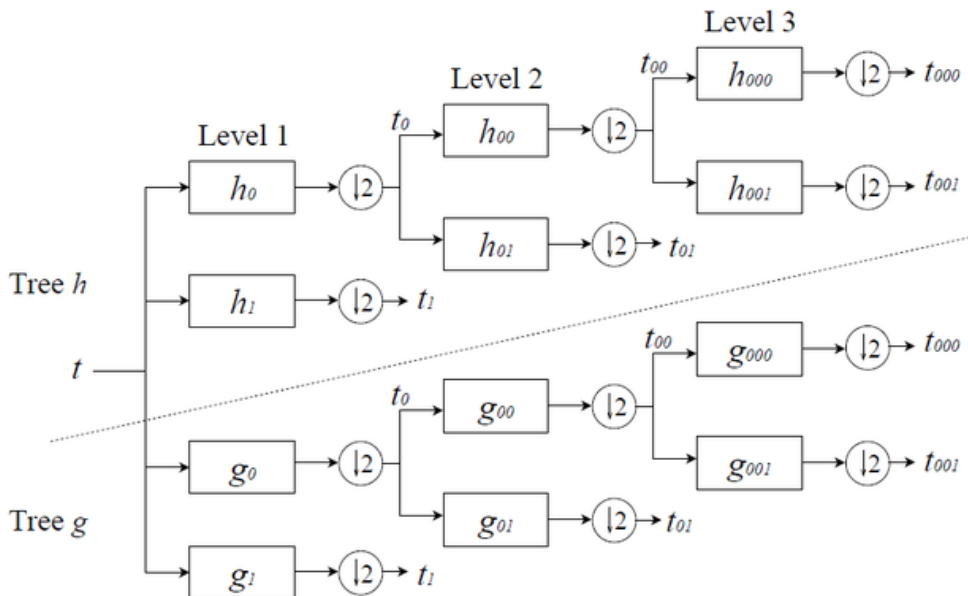
$$\angle d_c(s, t) = \arctan\left(\frac{d_h(s, t)}{d_g(s, t)}\right) \tag{7}$$

A coefficient with a high magnitude value represents a region in the signal with some kind of singularity such as, for example, an abrupt transition of the measured values.

The DT-CWT implementation uses a dual tree representation, with two DWT transforms. The first DWT results in the real part of the complex transform and the second results in the imaginary part. The mother wavelet functions $(\Psi_h(t))$ and $\Psi_g(t)$ of each of the DWTs are designed together to ensure that one is approximately the Hilbert transform of the other, that is, $\Psi_h(t) \approx \mathcal{H}(\Psi_g(t))$, and to ensure that the aliasing effect on a branch of the first tree (tree h) is approximately canceled with the corresponding branch on the second tree (tree g).

Figure 9 illustrates the decomposition scheme of a one-dimensional signal t using the double tree structure of DT-CWT. Although the scheme corresponds to a one-dimensional signal, it can be generalized to higher dimensions.

Figure 9. Three-level DT-CWT decomposition scheme using dual tree representation for an input signal t (Wang et al., 2021)



The real filters h_{s_0} and h_{s_0} represent the first pair of quadrature filters and the real filters g_{s_0} and g_{s_0} represent the second pair. Filters with index endings equal to 0 are low-pass filters, while filters with indexes ending in 1 represent high-pass filters (some of them are useful to the output of a low-pass filter from the previous level).

Statistical Feature Extraction by Principal Component Analysis (PCA) and Normalized Correlation

Principal Component Analysis

PCA is a linear combination of weights of the variables originally observed in the problem under analysis and that allows a better understanding of the observed data set and the reduction of the number of variables presented (Yücelbaş et al., 2018; Lastre-Domínguez et al., 2018).

However, the synthesis of how PCA is performed can be exemplified, according to the desired application in this work, as follows (Raghu & Sriraam, 2018):

- From an initial data matrix “ X ” formed by “ p ” morphological descriptors obtained from “ n ” ECG signals, as seen in equation (8):

$$X = \begin{bmatrix} x_{11} & x_{12} & \dots & x_{1p} \\ x_{21} & x_{22} & \dots & x_{2p} \\ \cdot & \cdot & \cdot & \cdot \\ \cdot & \cdot & \cdot & \cdot \\ \cdot & \cdot & \cdot & \cdot \\ x_{n1} & x_{n2} & \dots & x_{np} \end{bmatrix} \quad (8)$$

- The random vector “ x ” is considered to represent the set of descriptors selected for analysis, as seen in equation (9):

$$\vec{x} = [x_1, x_2, \dots, x_p] \quad (9)$$

- The covariance matrix, or correlation, is calculated for all descriptors;
- And the eigenvalues “ λ ” and eigenvectors “ a ” of “ k ” principal components are obtained through mathematical development of the calculated matrix, whether it is covariance or correlation, as seen in equation (10):

$$\lambda = [\lambda_1, \lambda_2, \dots, \lambda_k] \text{ and } a = \begin{bmatrix} \vec{a}_1 \\ \vec{a}_2 \\ \cdot \\ \cdot \\ \cdot \\ \vec{a}_k \end{bmatrix} = \begin{bmatrix} a_{11} & a_{12} & \dots & a_{1p} \\ a_{21} & a_{22} & \dots & a_{2p} \\ \cdot & \cdot & \cdot & \cdot \\ \cdot & \cdot & \cdot & \cdot \\ \cdot & \cdot & \cdot & \cdot \\ a_{k1} & a_{k2} & \dots & a_{kp} \end{bmatrix} \quad (10)$$

- The eigenvectors are vectors with the weights of the linear combinations used to calculate the value of the principal components “ y ” and the eigenvalues are the value of the variance of each principal component, that is, they indicate the representativeness of each calculated component, as seen in equation (11):

$$\begin{aligned} y_1 &= a_1 x = a_{11} x_1 + a_{12} x_2 + \dots + a_{1p} x_p \\ y_2 &= a_2 x = a_{21} x_1 + a_{22} x_2 + \dots + a_{2p} x_p \\ &\dots \\ y_k &= a_k x = a_{k1} x_1 + a_{k2} x_2 + \dots + a_{kp} x_p \end{aligned} \quad (11)$$

Therefore, for the example used, after performing PCA on a given set of descriptors, a new set of descriptors is obtained, composed of “ k ” elements. And these elements are the “ k ” principal components, also called factors, whose eigenvalue “ λ_k ” is the value of the variance presented by the factor “ y_k ” and the sum of the eigenvalues, $\sum_{i=0}^k \lambda_i$, is used to indicate the representativeness of the obtained set.

Normalized Correlation

It is a method for measuring the similarity between two signals or images. In most applications, these signals can still be considered very similar if the difference or ratio between the signals is constant. The purpose of normalization is to eliminate the effect of signals whose difference or ratio is constant, on the correlation value of these differences (Jha & Kolekar, 2020).

Normalized correlation can be defined as in equation (12).

$$NC = \frac{\sum_{i=1}^{M_1} \sum_{j=1}^{M_2} W(i, j) - W'(i, j)}{\sqrt{\sum_{i=1}^{M_1} \sum_{j=1}^{M_2} [W(i, j)]^2} \sqrt{\sum_{i=1}^{M_1} \sum_{j=1}^{M_2} [W'(i, j)]^2}} \quad (12)$$

Here, W is the original signal, W' is the noisysignal, and M_1, M_2 is the size of the original and noisysignals respectively. The value of the normalized correlation (NC) ranges between 0 and 1 and is calculated using Equation (12).

Feature Fusion using Neighborhood Component Analysis (NCA)

The (NCA) is a technique used to reduce the dimensionality of data in machine learning. Let $T = \{(x_1, y_1), \dots, (x_i, y_i), \dots, (x_N, y_N)\}$ be a training set, where x_i is an observation containing d features, $y_i \in \{1, \dots, C\}$ the corresponding class and N the number of observations. In this formalism, the objective is to determine a vector w containing weight factors that express the statistical relevance of each feature, in order to select a subset of features that optimizes the classification performance using leave-one-out validation (Lastre-Domínguez et al., 2018; Raghu & Sriraam, 2018).

NCA makes use of the following metric, which is a weighted distance between two observations x_i and x_j , as seen in equation (42):

$$D_w(x_i, x_j) = \sum_{l=1}^d w_l^2 |x_{il} - x_{jl}| \quad (13)$$

Where w_l is the weight associated with the l^{th} feature. The classification performance is given by equation (14):

$$\zeta(w) = \frac{1}{N} \sum_i p_i = \frac{1}{N} \sum_i \sum_j y_{ij} p_{ij} \quad (14)$$

$$\text{With, } p_{ij} = \begin{cases} \frac{KD_w(x_i, x_j)}{\sum_{k \neq i} KD_w(x_i, x_k)} & \text{if } i \neq j \\ 0 & \text{if } i = j \end{cases}$$

Where, K is a kernel function.

In order to effectively select features and avoid data overfitting, a regularization term λ is included in the following equation (15).

$$\zeta(w) = \sum_i \sum_j y_{ij} p_{ij} - \lambda \sum_{l=1}^d w_l^2 \quad (15)$$

As this function is differentiable, the derivative with respect to w_l can be computed to obtain equation (16):

$$\frac{\partial \zeta(w)}{\partial w_l} = 2w_l \left[\frac{1}{\sigma} \sum_i \left\{ p_i \sum_{j \neq i} p_{ij} |x_{il} - x_{jl}| - \sum_j y_{ij} p_{ij} |x_{il} - x_{jl}| \right\} - \lambda \right] \quad (16)$$

The discretization of the previous equation leads to an iterative algorithm that allows obtaining a vector containing weight factors for each feature and thus selecting features.

Classification by Support Vector Machines (SVM)

The SVM comes under the category of linear classifiers. A binary classification problem can be formalized as follows: given a set of points (x_i, y_i) , $i = 1, \dots, l$ where $x_i \in \mathbb{R}^d$ are feature vectors and $y_i \in \{-1, 1\}$ are classes, build a rule that correctly assigns a new point x to one of the classes. A binary classifier is then an application of the type: $f(x) : \mathbb{R}^d \rightarrow \{-1, 1\}$. As seen in equation (17), a classifier is linear if:

$$f(x; w, b) = \langle w, x \rangle + b \tag{17}$$

Where, w and b are classifier parameters and $\langle \cdot, \cdot \rangle$ designates the inner product of two vectors if there is a linear classifier such that: $y_i f(x_i) > 0$, for all $i = 1, \dots, l$.

Linear classifiers have their genesis in the perceptron algorithm. This algorithm starts by predicting the classes of each observation. If at least one of the predictions fails the parameters w and b of the hyperplane are readjusted, that is, they are shifted towards the point (observation) where the error occurred. The speed with which these parameters are shifted is dependent on another parameter called the learning rate, a parameter that increases significantly with the number of iterations until there is convergence (Jha & Kolekar, 2020).

The perceptron is a graph with weighted nodes and interconnections, as in a network of neurons. There are then two layers of nodes: an input layer and an output layer. The input layer has a node for each feature and an additional node equal to 1. The output layer consists of a single node, and each node of the inner layer is connected to the outer layer (Jha & Kolekar, 2020).

The motto of SVMs resides in Novikov's Theorem. Before stating this theorem, it is important to define the concept of margin. Consider a hyperplane $\langle w^*, x \rangle + b^*$, $\|w^*\| = 1$. If the condition $y_i (\langle w^*, x \rangle + b^*) \geq \gamma$ is satisfied for all points (x_i, y_i) in a training set S , the hyperplane is said to be separable with margin γ . Any separable hyperplane can be converted to the form: $y (\langle w, x \rangle + b) \geq 1$. So doing $\|w^*\| = w / \|w\|$ and $b^* = b / \|w\|$ a separable hyperplane with margin $\gamma = 1 / \|w\|$ is obtained.

We are in a position to state Novikov's Theorem. Let S , $|S| = l$ be a training set and let $R = \max \|x_i\|$. Suppose there is a hyperplane (w, b) such that $y_i (\langle w, x_i \rangle + b) \geq \gamma$, for all $i = 1, \dots, l$. then the maximum number of errors made by the perceptron algorithm in S is at most given by

$$\left(\frac{2R}{\gamma} \right)^2.$$

The probability of making a mistake is inversely proportional to the margin value. Therefore, in an SVM, the objective is to build a perceptron with the largest possible margin (in order to minimize the number of errors made), and that still manages to separate the points of the training set. This translates into the following optimization problem, as seen in equation (18):

$$\text{minimize}_{w,b} \langle w, w \rangle \text{ such that } y_i (\langle w, x_i \rangle + b) \geq 1, \text{ for all } i = 1, \dots, l \tag{18}$$

Problems of this type can be solved using Lagrange multipliers, α_i . In this case the Lagrangian function is given by, equation (19):

$$L(w, b, \alpha) = \frac{1}{2} \langle w, w \rangle - \sum_{i=1}^l \alpha_i \left[y_i (\langle w, x_i \rangle + b) - 1 \right] \quad (19)$$

Differentiating in order α , w and b gives equation (20):

$$w = \sum_{i=1}^l y_i \alpha_i x_i \text{ and } b = \sum_{i=1}^l y_i \alpha_i \quad (20)$$

Given the first condition in (19), an SVM can be defined, as seen in equation (21):

$$f(x) = \sum_{i=1}^l y_i \alpha_i \langle x_i, x \rangle + b \quad (21)$$

Until now, only linearly separable points have been considered. However, SVM can be reformulated to handle points that are not linearly separable, this is done by introducing slack variables (ζ) that control how far a point is on the wrong side of the hyperplane. The optimization problem is then reformulated as follows (Daqrouq & Dobaie, 2016):

$$\text{minimize}_{w,b} \left(\frac{1}{2} \langle w, w \rangle + c \sum_{i=1}^l \zeta_i \right)$$

Such that, it results in equation (22):

$$y_i (\langle w, x_i \rangle + b) \geq 1 - \zeta_i, \zeta_i \geq 0 \forall_i = 1, \dots, l \quad (22)$$

The C parameter controls the trade-off between the margin value and the training errors.

The SVM (which is a linear classifier) can be made nonlinear (in the original space) by introducing a function or kernel into the classifier expression. Common kernels include polynomials and Gaussian functions. We then obtain a classifier of the type, as seen in equation (23) (Jha & Kolekar, 2020):

$$f(x) = \sum_{i=1}^l y_i \alpha_i K(x_i, x) \quad (23)$$

RESULTS AND DISCUSSION

Evaluation Parameters

To evaluate the performance of the classification model, sensitivity, precision, specificity and accuracy were used as performance criteria. The success of the model is related to the number of correctly classified samples and incorrectly classified samples. According to the performance information obtained as a result of the test, these criteria are calculated according to the equations (24), (25), (26) and (27) below.

$$Accuracy = \frac{TP + TN}{TP + TN + FP + FN} \quad (24)$$

$$Precision = \frac{TP}{TP + FP} \quad (25)$$

$$Specificity = \frac{TN}{TN + FP} \quad (26)$$

$$Sensitivity = \frac{TP}{TP + FN} \quad (27)$$

Dataset

The dataset includes ECG data from three groups of subjects: subjects with abnormal heart rhythm (ARR) (96 recordings), congestive heart failure (CHF) (30 recordings), and subjects with normal sinus rhythm (NSR) (36 recordings). A total of, 162 ECG recordings were used three PhysioNet databases: MIT-BIH Arrhythmia Database (Goldberger et al., 2000), MIT-BIH Normal Sinus Rhythm Database (Vieau & Iaizzo, 2015), and The BIDMC Congestive Heart Failure Database (Pereira et al., 2020). Here the SVM classifier can distinguish between ARR, CHF, and NSR.

Simulation Results

The simulation results are performed on MATLAB 2019a. The process of training comprises of training signals and validation signals as shown in Table 1.

ECG signals can be used to analyze arrhythmias (ARR). It is a measure of heart rate and mood. Congestive heart failure (CHF) is a clinical condition in which the heart is unable to draw out blood at the rate necessary to contract tissues, or at the rate at which the heart fills with weight. NSR is used to denote a particular type of sinus musicality when all other ECG scores also fall within the commonly defined cut-points as shown in Figure 10 (ARR, CHF and NSR waveforms).

There are many CNN-based methods that have different architectural structures and are used in learning applications. The most common CNN architectures used in deep learning applications are AlexNet and GoogLeNet networks. Following are the results for AlexNet architecture.

The ECG signal training process is accomplished with 130 training signals and 32 validation signals as shown Figure 12 and 13.

Table 1. Process of training consisting of training signals and validation signals

Epoch	Iteration	Time Elapsed (hh:mm:ss)	Mini-batch Accuracy	Validation Accuracy	Mini-batch Loss	Validation Loss	Base Learning Rate
1	1	00:00:05	26.67%	47.22%	2.3848	1.2520	1.0000e-04
2	10	00:00:27	60%	63.89%	1.3482	0.9712	1.0000e-04
3	20	00:00:52	66.67%	72.22%	1.0305	0.6557	1.0000e-04
4	30	00:01:16	66.67%	80.56%	0.5623	0.4883	1.0000e-04
5	40	00:01:40	60%	83.33%	0.7282	0.4268	1.0000e-04
7	50	00:02:05	100%	77.78%	0.1406	0.4307	1.0000e-04
8	60	00:02:29	73.33%	83.33%	0.5192	0.3589	1.0000e-04
9	70	00:02:54	100%	88.89%	0.2178	0.2984	1.0000e-04
10	80	00:03:15	86.67%	91.67%	0.2329	0.2784	1.0000e-04
12	90	00:03:37	93.33%	91.67%	0.2039	0.2564	1.0000e-04
13	100	00:03:58	86.67%	94.44%	0.2575	0.2304	1.0000e-04
14	110	00:04:20	100%	97.22%	0.1126	0.2027	1.0000e-04
15	120	00:04:41	86.67%	97.22%	0.4469	0.1941	1.0000e-04
17	130	00:05:02	100%	97.22%	0.1477	0.1624	1.0000e-04
18	140	00:05:23	93.33%	97.22%	0.1482	0.1668	1.0000e-04
19	150	00:05:44	93.33%	94.44%	0.1889	0.2053	1.0000e-04
20	160	00:06:05	93.33%	97.22%	0.2463	0.1308	1.0000e-04

Figure 10. Input ECG signal with ARR, CHF and NSR

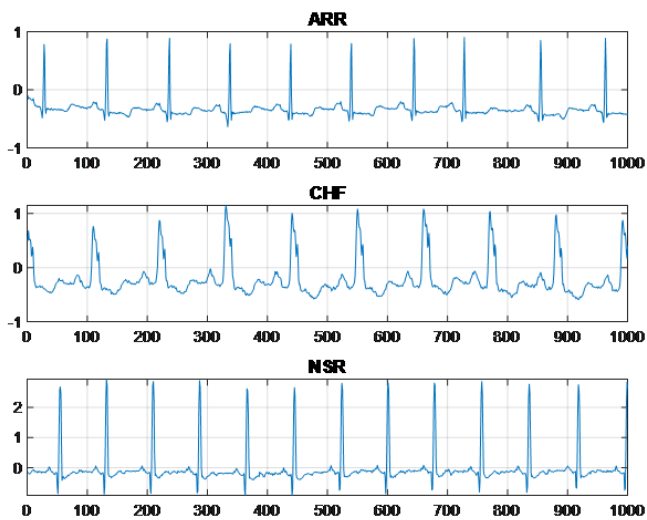


Figure 11. ECG scalogram using CWT

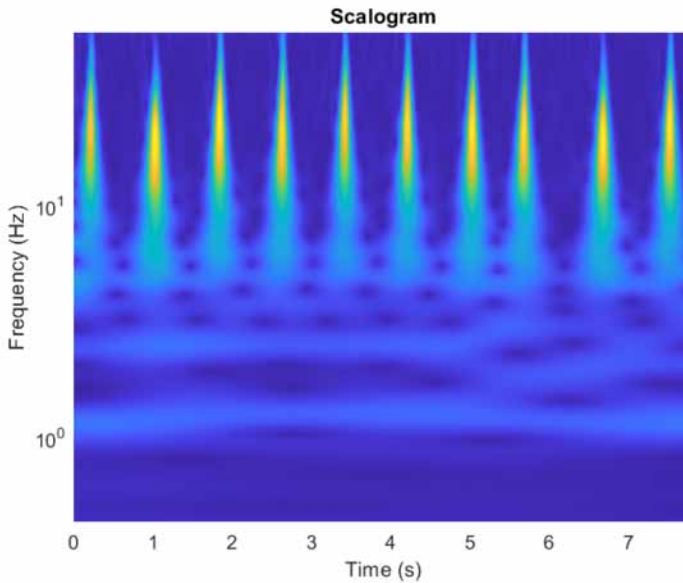


Figure 12. AlexNet based deep learning network analysis result-1

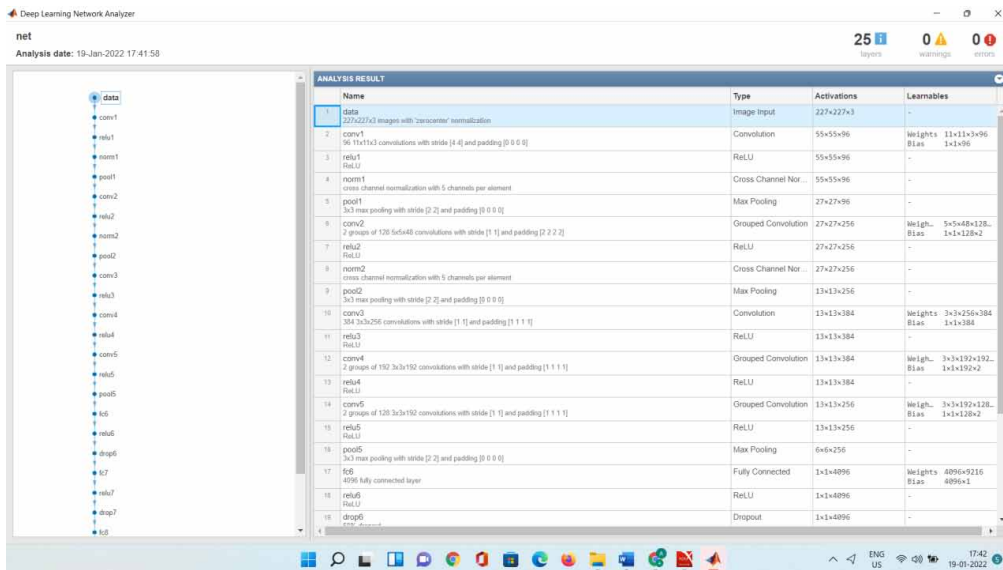


Table 2 represents the confusion matrix of AlexNet CNN where three class output is defined as predicted class 1, predicted class 2 and predicted class 3 respectively. It can be observed that there are total 19 samples available in class1 but 18 predicted properly and 1 misclassified as class 2. Class 3 gives 100% accuracy as all the classes are predicted correctly. Table 3 represents the True Positive, False Positive, False Negative and True Negative values.

Figure 13. AlexNet based deep learning network analysis result-2

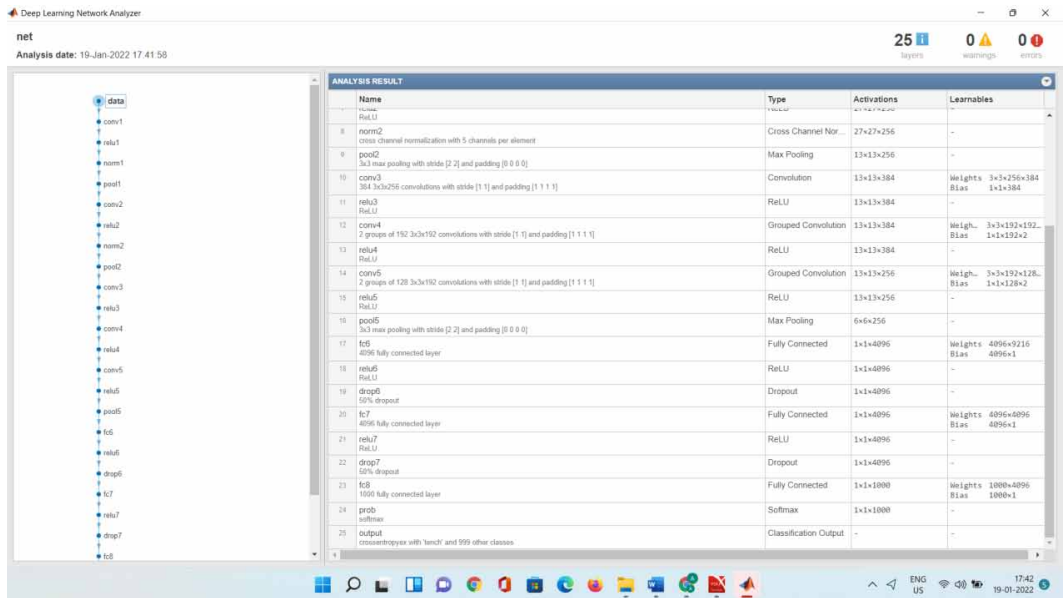


Table 2. Confusion Matrix using AlexNet CNN

Classes	Predict Class 1	Predict Class 2	Predict Class 3
Actual Class 1	18	2	0
Actual Class 2	1	4	0
Actual Class 3	0	0	7

Table 3. Multi-Class Confusion Matrix Output using AlexNet CNN

Classes	True Positive	False Positive	False Negative	True Negative
Actual Class 1	18	1	2	11
Actual Class 2	4	2	1	25
Actual Class 3	7	0	0	25

Table 4 shows the classification results for three different PhysioNet datasets trained using different sets of feature vectors. The AlexNet-based CNN system model achieves an efficiency of 90.63% for three-class classification using a support vector classifier, while the overall accuracy of the proposed approach using GoogLeNet’s (ARR, CHF and NSR) three-class CNN architecture is 97.22%. With the NCA-based feature set system model, the mean statistic F1-score, MCC, and kappa score were higher (88.34%, 82.68%, and 78.91%). A higher F-score indicates a better ranking in the classifier.

A comparison of the proposed design with the available techniques for the three reference datasets is presented in Table 5. The proposed model is a three-class hit classification structure estimated from a feature-based fusion dataset. This far outstripped previous work at the NCA, where the proposed setup achieved an accuracy of 90.63% and 97.22%, respectively.

Table 4. Final Results using AlexNet CNN

Parameter	Result
Accuracy	0.9063
Error	0.0938
Sensitivity	0.9000
Specificity	0.9475
Precision	0.8713
False Positive Rate	0.0525
F1-Score	0.8834
Matthews Correlation Coefficient	0.8268
Kappa	0.7891

Table 5. Comparison of result with previous research works

Reference No.	Method used	Class	Accuracy performance
Daqrouq and Dobaie (2016)	Feature extraction using wavelet packet transform and classification by confirmation functions	2 (CHF,NSR)	92.60%
Nahak and Saha (2020)	Feature fusion and classification with SVM	3 (ARR,CHF,NSR)	93.33%
Sandeep et al. (2019)	Wavelet based feature extraction and classification using CNN	3 (ARR,CHF,NSR)	90.63%
Çinar and Tuncer (2021)	hybrid CNN-SVM deep neural networks	3 (ARR,CHF,NSR)	96.77%
Proposed Method	Using AlexNet CNN	3 (ARR,CHF,NSR)	90.63%
Proposed Method	Using Google Net CNN	3 (ARR,CHF,NSR)	97.22%.

CONCLUSION

In this article, a new ECG classification technique is developed based on combining NCA-based deep features, morphological features, DT-CWT-based features, and statistical features using PCA and normalized correlations. To avoid the overlap effect of various frequency components, CWT was initially utilized to convert the ECG heartbeat signal into the time-frequency domain. The CNN was then utilized to extract features from the scalogram consisting of time-frequency decomposition components, after which the methods mentioned above for other features were applied. This method can take full advantage of CNN in image recognition and CWT in multivariate signal processing. When tested against the PhysioNet database, the SVM classifier with AlexNet CNN showed overall performance of 5.25%, 90%, 94.75%, 88.34%, and 90.63% for false positive rate, sensitivity, specificity, F1-score, and accuracy obtained in any case. In addition, GoogleNet CNN with SVM classifier offers a maximum accuracy of 97.22%, which is significantly higher than previous studies. This approach can be utilized as a supplementary clinical diagnostic tool due to the higher accuracy of classification of ECG signal. In general, early diagnosis of cardiac arrhythmias is necessary as the main cause of cardiovascular diseases. After appropriate early diagnosis, effective treatment such as medications or vagal maneuvers can decrease arrhythmias and prevent cardiovascular disease. This performance can be improved using different biological signals, and classification performance can be compared with different CNN architectures. The quantity of data points used and the number of diseases will

be enhanced in future studies. Furthermore, the impact of this condition on the suggested hybrid CNN architecture will be investigated.

CONFLICT OF INTEREST

The authors declare no conflict of interest.

FUNDING INFORMATION

No funding

REFERENCES

- Alarsan, F. I., & Younes, M. (2019, August). Analysis and classification of heart diseases using heartbeat features and machine learning algorithms. *Journal of Big Data*, 6(1), 81. doi:10.1186/s40537-019-0244-x
- Anwar, S. M., Gul, M., Majid, M., & Alnowami, M. (2018, November). Arrhythmia classification of ECG signals using hybrid features. *Computational and Mathematical Methods in Medicine*, 1380348, 1–8. Advance online publication. doi:10.1155/2018/1380348 PMID:30538768
- Bulbul, H. I., Usta, N., & Yildiz, M. (2017, December 18–21). Classification of ECG arrhythmia with machine learning techniques. In *2017 16th IEEE International Conference on Machine Learning and Applications (ICMLA)* (pp. 546–549). IEEE. doi:10.1109/ICMLA.2017.0-104
- Chen, H., & Maharatna, K. (2020, October). An automatic R and T peak detection method based on the combination of hierarchical clustering and discrete wavelet transform. *IEEE Journal of Biomedical and Health Informatics*, 24(10), 2825–2832. doi:10.1109/JBHI.2020.2973982 PMID:32078569
- Çınar, A., & Tuncer, S. A. (2021, February). Classification of normal sinus rhythm, abnormal arrhythmia and congestive heart failure ECG signals using LSTM and hybrid CNN-SVM deep neural networks. *Computer Methods in Biomechanics and Biomedical Engineering*, 24(2), 203–214. doi:10.1080/10255842.2020.1821192 PMID:32955928
- Daqrouq, K., & Dobaie, A. (2016, February). Wavelet based method for congestive heart failure recognition by three confirmation functions. *Computational and Mathematical Methods in Medicine*, 7359516, 1–11. Advance online publication. doi:10.1155/2016/7359516 PMID:26949412
- Desai, U., Martis, R. J., Nayak, C. G., Sarika, K., & Seshikala, G. (2015, 17–20 Dec.). Machine intelligent diagnosis of ECG for arrhythmia classification using DWT, ICA and SVM techniques. In *2015 Annual IEEE India Conference (INDICON)*, New Delhi, India (pp. 1–4). IEEE. doi:10.1109/INDICON.2015.7443220
- Dewangan, N. K., & Shukla, S. P. (2016, May 20–21). ECG arrhythmia classification using discrete wavelet transform and artificial neural network. In *2016 IEEE International Conference on Recent Trends in Electronics, Information & Communication Technology (RTEICT)* (pp. 1892–1896). IEEE. doi:10.1109/RTEICT.2016.7808164
- Dössel, O., Luongo, G., Nagel, C., & Loewe, A. (2021, July). Computer Modeling of the heart for ECG interpretation—A review. *Hearts*, 2(3), 350–368. doi:10.3390/hearts2030028
- Goldberger, A. L., Amaral, L. A., Glass, L., Hausdorff, J. M., Ivanov, P. C., Mark, R. G., Mietus, J. E., Moody, G. B., Peng, C. K., & Stanley, H. E. (2000, June). PhysioBank, PhysioToolkit, and PhysioNet: Components of a new research resource for complex physiologic signals. *Circulation*, 101(23), e215–e220. doi:10.1161/01.CIR.101.23.e215 PMID:10851218
- Goldberger, A. L., Goldberger, Z. D., & Shvilkin, A. (2018). Section 2- Supplemental Extras. In *Goldberger's Clinical Electrocardiography: A Simplified Approach* (9th ed., pp. e54–e71). Elsevier. doi:10.1016/B978-0-323-40169-2.00027-5
- Hamed, I., & Owis, M. I. (2016). Automatic arrhythmia detection using support vector machine based on discrete wavelet transform. *Journal of Medical Imaging and Health Informatics*, 6(1), 204–209. doi:10.1166/jmihi.2016.1611
- Hannun, A. Y., Rajpurkar, P., Haghpanahi, M., Tison, G. H., Bourn, C., Turakhia, M. P., & Ng, A. Y. (2019, March). Cardiologist-level arrhythmia detection and classification in ambulatory electrocardiograms using a deep neural network. *Nature Medicine*, 25(3), 530. doi:10.1038/s41591-019-0359-9 PMID:30679787
- Hatami, N., Gavet, Y., & Debayle, J. (2018, April 13). Classification of time-series images using deep convolutional neural networks. In *Tenth international conference on machine vision (ICMV 2017)* (Vol. 10696, p. 106960Y). International Society for Optics and Photonics. doi:10.1117/12.2309486
- Huang, J., Chen, B., Yao, B., & He, W. (2019, July). ECG arrhythmia classification using STFT-based spectrogram and convolutional neural network. *IEEE Access: Practical Innovations, Open Solutions*, 7, 92871–92880. doi:10.1109/ACCESS.2019.2928017
- Inis, A., & Ozdalili, S. (2017). Cardiac arrhythmia detection using deep learning. *Procedia Computer Science*, 120, 268–275. doi:10.1016/j.procs.2017.11.238

- Islar, Y. (2016, September). Discrimination of systolic and diastolic dysfunctions using multi-layer perceptron in heart rate variability analysis. *Computers in Biology and Medicine*, 76, 113–119. doi:10.1016/j.combiomed.2016.06.029 PMID:27424172
- Izci, E., Ozdemir, M. A., Sadighzadeh, R., & Akan, A. (2018, 8-10 Nov.). Arrhythmia detection on ECG signals by using empirical mode decomposition. In 2018 Medical Technologies National Congress (TIPTEKNO), Magusa, Cyprus (pp. 1-4). IEEE. doi:10.1109/TIPTEKNO.2018.8597094
- Jha, C. K., & Kolekar, M. H. (2020, May). Cardiac arrhythmia classification using tunable Q-wavelet transform based features and support vector machine classifier. *Biomedical Signal Processing and Control*, 59, 101875. doi:10.1016/j.bspc.2020.101875
- JunT. J.NguyenH. M.KangD.KimD.KimY. H. (2018). *ECG arrhythmia classification using a 2-D convolutional neural network*. arXiv:1804.06812v1 [cs.CV]
- Kiranyaz, S., Ince, T., & Gabbouj, M. (2016, March). Real-time patient-specific ECG classification by 1-D convolutional neural networks. *IEEE Transactions on Biomedical Engineering*, 63(3), 664–675. doi:10.1109/TBME.2015.2468589 PMID:26285054
- Kurniawan, A., Ananda, Pradanggapasti, F. N., Rachmadi, R. F., Setijadi, E., Yuniarno, E. M., Yusuf, M., & Purnama, I. K. E. (2020, November 17-18). Arrhythmia Classification on Electrocardiogram Signal Using Convolution Neural Network Based on Frequency Spectrum. In 2020 International Conference on Computer Engineering, Network, and Intelligent Multimedia (CENIM), Surabaya, Indonesia (pp. 29-33). IEEE. doi:10.1109/CENIM51130.2020.9297997
- Kusumoto, F. M., & Bernath, P. (2012). *ECG interpretation for everyone: An on-the-spot guide*. Wiley-Blackwell.
- Lastre-Domínguez, C., Shmaliy, Y. S., Ibarra-Manzano, O., Munoz-Minjarez, J., & Vazquez-Olguin, M. (2018, November 14-16). Fiducial features extraction for ECG signals using state-space unbiased FIR smoothing. In 2018 IEEE International Autumn Meeting on Power, Electronics and Computing (ROPEC), Ixtapa, Mexico (pp. 1-6). IEEE. doi:10.1109/ROPEC.2018.8661460
- Li, H., Wei, X., Zuo, S., Dou, Q., Ding, M., Cao, L., Gong, Z., Wang, R., Chen, X., Wang, B., Prades, J. D., & Wu, F. (2020, January). Arrhythmia classification algorithm based on multi-feature and multi-type optimized SVM. *American Academic Scientific Research Journal for Engineering, Technology, and Sciences*, 63(1), 72–86.
- Manik, A., Adiwijaya, A., & Utama, D. (2019, April 12). Classification of Electrocardiogram Signals using Principal Component Analysis and Levenberg Marquardt Backpropagation for Detection Ventricular Tachyarrhythmia. *Journal of Data Science and Its Applications*, 2(1), 29–37. doi:10.21108/jdsa.2019.2.12
- Masetic, Z., & Subasi, A. (2016, July). Congestive heart failure detection using random forest classifier. *Computer Methods and Programs in Biomedicine*, 130, 54–64. doi:10.1016/j.cmpb.2016.03.020 PMID:27208521
- Nahak, S., & Saha, G. (2020, February 21-23). A fusion based classification of normal, arrhythmia and congestive heart failure in ECG. In 2020 National Conference on Communications (NCC), Kharagpur, India (pp. 1-6). IEEE. doi:10.1109/NCC48643.2020.9056095
- Nonaka, N., & Seita, J. (2020). *Data augmentation for electrocardiogram classification with deep neural network*. arXiv:2009.04398v1. <https://doi.org/10.48550/arXiv.2009.04398>.
- Pereira, R. M., Bispo, B. C., & Rodrigues, P. M. (2020, April). Heart disease detection using ECG lead I and multiple pattern recognition classifiers. *IOSR Journal of Engineering*, 10(4), 1–8.
- Pokaprakarn, T., Kitzmiller, R. R., Moorman, R., Lake, D. E., Krishnamurthy, A. K., & Kosorok, M. R. (2022, February). Sequence to Sequence ECG Cardiac Rhythm Classification using Convolutional Recurrent Neural Networks. *IEEE Journal of Biomedical and Health Informatics*, 26(2), 572–580. doi:10.1109/JBHI.2021.3098662 PMID:34288883
- Qaisar, S. M., Krichen, M., & Jallouli, F. (2020, June). Multirate ECG processing and k-nearest neighbor classifier based efficient arrhythmia diagnosis. In *18th International Conference on Smart Homes and Health Telematics (ICOST 2020), Hammamet, Tunisia, June 24–26, The Impact of Digital Technologies on Public Health in Developed and Developing Countries* (pp. 329-337). Springer. doi:10.1007/978-3-030-51517-1_29

- Raghu, S., & Sriraam, N. (2018, December). Classification of focal and non-focal EEG signals using neighborhood component analysis and machine learning algorithms. *Expert Systems with Applications*, 113, 18–32. doi:10.1016/j.eswa.2018.06.031
- Sandeep, K., Kora, P., Swaraja, K., Meenakshi, K., & Pampana, L. K. (2019, November). ECG classification using machine learning. *International Journal of Recent Technology and Engineering*, 8(4), 2492–2494. doi:10.35940/ijrte.D6989.118419
- Sharma, A., Garg, N., Patidar, S., Tan, R. S., & Acharya, U. R. (2020, May). Automated pre-screening of arrhythmia using hybrid combination of Fourier–Bessel expansion and LSTM. *Computers in Biology and Medicine*, 120, 103753. doi:10.1016/j.combiomed.2020.103753 PMID:32421653
- Singh, N., & Singh, P. (2019). Cardiac arrhythmia classification using machine learning techniques. In *Engineering Vibration, Communication and Information Processing, Lecture Notes in Electrical Engineering* (vol 478, pp. 469–480). Springer. doi:10.1007/978-981-13-1642-5_42
- Singh, S. A., & Majumder, S. (2019, June). A novel approach for arrhythmia detection using single-lead ECG scalogram based on deep neural network. *Journal of Mechanics in Medicine and Biology*, 19(04), 1950026. doi:10.1142/S021951941950026X
- Subbiah, S., & Subramanian, S. (2018). Biomedical arrhythmia heart diseases classification based on artificial neural network and machine learning approach. *International Journal of Engineering and Technology*, 7(3.27), 10–14. 10.14419/ijet.v7i3.27.17642
- Ullah, A., Anwar, S. M., Bilal, M., & Mehmood, R. M. (2020, May). Classification of arrhythmia by using deep learning with 2-D ECG spectral image representation. *Remote Sensing*, 12(10), 1685. doi:10.3390/rs12101685
- Vieau, S., & Iaizzo, P. A. (2015). Basic ECG theory, 12-lead recordings, and their interpretation. In P. A. Iaizzo (Ed.), *Handbook of Cardiac Anatomy, Physiology, and Devices* (pp. 321–334). Springer. doi:10.1007/978-3-319-19464-6_19
- Wang, T., Lu, C., Sun, Y., Yang, M., Liu, C., & Ou, C. (2021, January). Automatic ECG classification using continuous wavelet transform and convolutional neural network. *Entropy (Basel, Switzerland)*, 23(1), 119. doi:10.3390/e23010119 PMID:33477566
- Xiang, Y., Luo, J., Zhu, T., Wang, S., Xiang, X., & Meng, J. (2018). ECG-based heartbeat classification using two-level convolutional neural network and RR interval difference. *IEICE Transactions on Information and Systems*, E101.D(4), 1189–1198. 10.1587/transinf.2017EDP7285
- Xiong, Z., Nash, M. P., Cheng, E., Fedorov, V. V., Stiles, M. K., & Zhao, J. (2018, September). ECG signal classification for the detection of cardiac arrhythmias using a convolutional recurrent neural network. *Physiological Measurement*, 39(9), 094006. doi:10.1088/1361-6579/aad9ed PMID:30102248
- Yıldırım, Ö., Pławiak, P., Tan, R. S., & Acharya, U. R. (2018). Arrhythmia detection using deep convolutional neural network with long duration ECG signals. *Computers in Biology and Medicine*, 102, 411–420. 10.1016/j.combiomed.2018.09.009
- Yücelbaş, Ş., Yücelbaş, C., Tezel, G., Özşen, S., & Yosunkaya, Ş. (2018, July). Automatic sleep staging based on SVD, VMD, HHT and morphological features of single-lead ECG signal. *Expert Systems with Applications*, 102, 193–206. doi:10.1016/j.eswa.2018.02.034
- Zhang, J., Liu, A., Gao, M., Chen, X., Zhang, X., & Chen, X. (2020). ECG-based multi-class arrhythmia detection using spatio-temporal attention-based convolutional recurrent neural network. *Artificial Intelligence in Medicine*, 106, 101856. 10.1016/j.artmed.2020.101856
- Zhao, Y., Cheng, J., Zhang, P., & Peng, X. (2020, June). ECG classification using deep CNN improved by wavelet transform. *Computers. Materials and Continua*, 64(3), 1615–1628. doi:10.32604/cmc.2020.09938